Published in final edited form as:
*Eur J Pharmacol*. 2007 August 13; 569(1-2): 48–58.

# A peroxynitrite decomposition catalyst counteracts sensory neuropathy in streptozotocin-diabetic mice

**Viktor R. Drel**[a], **Pal Pacher**[b], **Igor Vareniuk**[a], **Ivan Pavlov**[a], **Olga Ilnytska**[a], **Valeriy V. Lyzogubov**[a], **Jyoti Tibrewala**[c], **John T. Groves**[c], and **Irina G. Obrosova**[a,*]

a *Pennington Biomedical Research Center, Louisiana State University System, Baton Rouge, LA, United States*

b *Section on Oxidative Stress Tissue Injury, Laboratory of Physiological Studies, NIH/NIAAA, Bethesda, MD, United States*

c *Department of Chemistry, Princeton University, Princeton, NJ, United States*

## Abstract

Whereas an important role of free radicals and oxidants in peripheral diabetic neuropathy is well established, the contribution of nitrosative stress and, in particular, of the highly reactive oxidant peroxynitrite, has not been properly explored. Our previous findings implicate peroxynitrite in diabetes-associated motor and sensory nerve conduction deficits and peripheral nerve energy deficiency and poly(ADP-ribose) polymerase activation associated with Type 1 diabetes. In this study the role of nitrosative stress in diabetic sensory neuropathy is evaluated. The peroxynitrite decomposition catalyst Fe(III) tetrakis-2-(*N*-triethylene glycol monomethyl ether)pyridyl porphyrin (FP15) was administered to control and streptozotocin (STZ)-diabetic mice at the dose of 5 mg $kg^{-1}$ $day^{-1}$ (FP15), for 3 weeks after initial 3 weeks without treatment. Mice with 6-week duration of diabetes developed clearly manifest thermal hypoalgesia (paw withdrawal, tail-flick, and hot plate tests), mechanical hypoalgesia (tail pressure Randall–Sellito test), tactile allodynia (flexible von Frey filament test), and ~38% loss of intraepidermal nerve fibers. They also had increased nitrotyrosine and poly(ADP-ribose) immunofluorescence in the sciatic nerve, grey matter of spinal cord, and dorsal root ganglion neurons. FP15 treatment was associated with alleviation of thermal and mechanical hypoalgesia. Tactile response threshold tended to increase in response to peroxynitrite decomposition catalyst treatment, but still remained ~59% lower compared with non-diabetic controls. Intraepidermal nerve fiber density was 25% higher in FP15-treated than in untreated diabetic rats, but the difference between two groups did not achieve statistical significance ($p$=0.054). Nitrotyrosine and poly(ADP-ribose) immunofluorescence in sciatic nerve, spinal cord, and dorsal root ganglion neurons of peroxynitrite decomposition catalyst-treated diabetic mice were markedly reduced. In conclusion, nitrosative stress plays an important role in sensory neuropathy associated with Type 1 diabetes. The findings provide rationale for further studies of peroxynitrite decomposition catalysts in a long-term diabetic model.

### Keywords

Intraepidermal nerve fiber loss; Nitrosative stress; Peroxynitrite decomposition catalyst; Poly(ADP-ribose) polymerase; Tactile allodynia; Thermal hypoalgesia

* Corresponding author. Pennington Biomedical Research Center, Louisiana State University, 6400 Perkins Road, Baton Rouge, LA 70808, United States. Tel.: +1 225 763 0276; fax: +1 225 763 0274. E-mail address: obrosoig@pbrc.edu (I.G. Obrosova).

Evidence for important role of the potent oxidant peroxynitrite, a product of superoxide anion radicals with nitric oxide, in the pathogenesis of diabetes (Olcott et al., 2004; Szabo et al., 2002a; Pacher et al., 2007) and diabetic complications (Nangle et al., 2004; Obrosova et al., 2005b; Pacher et al., 2005; Pacher et al., 2007; Szabo et al., 2002a) is emerging. Accumulation of nitrotyrosine [NT, a footprint of peroxynitrite- and other reactive nitrogen species (RNS)-induced protein nitration] has been documented in vascular endothelium (Pacher et al., 2005; Szabo et al., 2002b), myocardium (Pacher et al., 2005), retina (Cheung et al., 2005; Obrosova et al., 2005c), and kidneys (Drel et al., 2006b) of streptozotocin-diabetic rats and mice as well as cutaneous microvascular endothelium (Szabo et al., 2002b), myocardium (Frustaci et al., 2000), and kidneys (Thuraisingham et al., 2000) of human subjects with diabetes. Increased NT immunoreactivity has also been demonstrated in peripheral nervous system *i.e.*, peripheral nerve, spinal cord and dorsal root ganglion (DRG) neurons, of STZ-diabetic rats (Cheng and Zochodne, 2003; Obrosova et al., 2005a) and STZ-diabetic (Ho et al., 2006; Obrosova et al., 2005b), *ob*/*ob* (Drel et al., 2006a), and high-fat diet fed mice (Obrosova et al., 2007b), and epineurial vessels of STZ-diabetic, ZDF diabetic fatty, and Zucker fatty rats (Coppey et al., 2001; Obrosova et al., 2005a,b; Oltman et al., 2005). Enhanced nitrosative stress has been reported in human subjects with peripheral diabetic neuropathy (Hoeldtke, 2003). Furthermore, increased nitrosylated protein abundance has been identified very early during exposure of cultured human Schwann cells to high glucose (Obrosova et al., 2005a).

The role of nitrosative component of free radical and oxidant-induced injury in peripheral diabetic neuropathy has not been properly explored. Two recent studies (Nangle et al., 2004; Obrosova et al., 2005b), including one from our group (Obrosova et al., 2005b), implicated peroxynitrite in motor and sensory nerve conduction deficits, thermal hypoalgesia, and impaired nitrergic innervation, known to contribute to autonomic neuropathy, in STZ-diabetic rats and mice and nonobese diabetic (NOD) mice. Here, we describe studies with a potent peroxynitrite decomposition catalyst which revealed an important role of nitrosative stress in diabetic sensory neuropathy. Our findings implicate RNS in thermal and mechanical hypoalgesia, tactile allodynia, intraepidermal nerve fiber loss, and poly(ADP-ribose) polymerase activation in peripheral nerve, grey matter of spinal cord, and DRG neurons and satellite cells in streptozotocin-diabetic mice. A peroxynitrite decomposition catalyst treatment reduced diabetes-associated nitrosative stress and PARP activation in tissue sites of peripheral diabetic neuropathy, and alleviated, but not completely prevented, dysfunction and degeneration of small sensory fibers.

## 1. Methods

### 1.1. Reagents

Unless otherwise stated, all chemicals were of reagent-grade quality, and were purchased from Sigma Chemical Co., St. Louis, MO. Fe(III) tetrakis-2-(*N*-triethylene glycol monomethyl ether)pyridyl porphyrin (FP15) was synthesized as previously described (Szabo et al., 2002a). Rabbit polyclonal anti-NT antibody was purchased from Upstate, Lake Placid, NY, and mouse monoclonal anti-poly(ADP-ribose) from Trevigen, Inc., Gaithersburg, MD. Secondary Alexa Fluor 488 goat anti-rabbit and Alexa Fluor 488 goat anti-mouse antibodies as well as Prolong Gold Antifade Reagent were purchased from Invitrogen, Eugene, OR. Avidin/Biotin Blocking Kit, M.O.M. Basic Kit, VECTASTAIN Elite ABC Kit (Standard*), DAB Substrate Kit, and 3,3′-diaminobenzidine were obtained from Vector Laboratories, Burlingame, CA. Rabbit polyclonal anti-protein gene product 9.5 (ubiquitin c-terminal hydrolase) antibody was purchased from Chemicon International, Inc, Temecula, CA. Other reagents for immunohistochemistry have been purchased from Dako Laboratories, Inc., Santa Barbara, CA.

### 1.2. Animals

The experiments were performed in accordance with regulations specified by the National Institutes of Health "Principles of Laboratory Animal Care, 1985 Revised Version" and Pennington Biomedical Research Center Protocol for Animal Studies. Mature male C57Bl6/J mice were purchased from Jackson Laboratories (Bar Harbor, ME). They were fed with standard mouse chow (PMI Nutrition International, Brentwood, MO) and had access to water *ad libitum*. Diabetes was induced by a single injection of streptozotocin (STZ, 100 mg $kg^{-1}$ $day^{-1}$, i.p.) to non-fasted animals. Blood samples for glucose measurements were taken from the tail vein 3 days after STZ injection and the day before the animals were killed. The mice with blood glucose ≥13.8 mM were considered diabetic. The injected mice that had blood glucose concentration in non-diabetic range have been given low-dose STZ injections (40 mg $kg^{-1}$ $day^{-1}$, i.p.) until they developed hyperglycemia (typically, one-three additional injections). The experimental groups comprised control and diabetic mice treated with or without the peroxynitrite decomposition catalyst Fe(III) tetrakis-2-(*N*-triethylene glycol monomethyl ether)pyridyl porphyrin (FP15) (Mabley et al., 2002; Szabo et al., 2002a; Obrosova et al., 2005b; Pacher et al., 2003). The agent was administered at the dose of 5 mg $kg^{-1}$ $day^{-1}$ (FP15), in the drinking water, for 3 weeks after initial 3 weeks without treatment. This dose was selected from our previous experiments in the same animal model (Obrosova et al., 2005b). At the 3-week time point and the end of the study, the physiological and behavioral tests have been performed in the following order: tactile responses to flexible von Frey filaments (first day), tail pressure Randall–Sellito test (second day), thermal algesia by tail-flick test (third day), thermal algesia by paw withdrawal test (fourth day), thermal algesia by hot plate test (sixth day). The mice with 3-week duration of STZ-diabetes displayed thermal hypoalgesia (paw withdrawal latencies: 15.56±0.61 s vs 10.36± 0.48 s in controls, $p<0.01$; tail-flick response latencies: 3.27± 0.12 s vs 2.8±0.08 s in controls, $p<0.01$), mechanical hypoalgesia (withdrawal threshold in the tail pressure Randall–Selitto test: 200±2.5 g vs 166 ±2.5 g in controls, $p<0.01$), tactile allodynia (tactile response threshold: 1.35±.10 g vs 2.23 ±0.26 g in controls, $p<0.05$), but no intraepidermal nerve fiber loss (23.2±2.3 nerve fiber profiles per mm vs 24.3±2.8 nerve fiber profiles per mm in controls).

### 1.3. Anesthesia, euthanasia and tissue sampling

The animals were sedated by $CO_2$, and immediately sacrificed by cervical dislocation. Sciatic nerves, spinal cord, DRGs, and foot pads were fixed in normal buffered 4% formalin for assessment of nitrotyrosine (NT) and poly(ADP-ribose) by immunofluorescent histochemistry and intraepidermal nerve fiber density by conventional immunohistochemistry.

### 1.4. Specific methods

#### 1.4.1. Behavioral tests

**1.4.1.1. Tactile responses and mechanical algesia:** Tactile responses were evaluated by quantifying the withdrawal threshold of the hindpaw in response to stimulation with flexible von Frey filaments as we have described (Ilnytska et al., 2006). Tail pressure thresholds were registered with the Paw/Tail Pressure Analgesia meter for the Randall–Selitto test [37215-Analgesy-Meter, UGO-Basile, Comerio VA, Italy]. Pressure increasing at a linear rate of 10 g $s^{-1}$ with the cut-off of 250 g to avoid tissue injury, was applied to the base of the tail. The applied tail pressure that evoked biting or licking behavior was registered by analgesia meter and expressed in g. Three tests separated by at least 15 min were performed for each animal, and the mean value of these tests was calculated.

**1.4.1.2. Thermal algesia:** The paw withdrawal latency in response to the radiant heat (15% intensity which produced a heating rate of ~1.3 °C per s, cut-off time 30 s) was determined as we have described (Ilnytska et al., 2006) using the IITC model 336 TG combination tail-flick

and paw algesia meter (IITC Life Science) with a floor temperature ~32–33 °C (manufacturer's set up). For assessment of tail-flick response latencies, the device was set at 40% heating intensity (heating rate ~2.5 °C per s) with a cut-off at 10 s. In the hot plate test (IITC Model 39 Hot Plate Analgesia Meter, IITC Life Science) the unit had a plate preset temperature of 55 °C. In all three tests, at least three readings per animal were taken at 15 min interval, and the average was calculated.

**1.4.2. Immunohistochemical studies—**All sections were processed by a single investigator and evaluated blindly. Low power observations of skin sections stained for PGP 9.5 were made using a Zeiss Axioskop microscope. Color images were captured with a Zeiss Axiocam HRc CCD camera at 1300×1030 resolution. Low power images were generated with a 40X acroplan objective using the automatic capturing feature of the Zeiss Axiovision software (Ver. 3.1.2.1). Low power observations of sciatic nerve, spinal cord and DRG sections stained for NT and poly(ADP-ribose) were made using a Zeiss Axioplan 2 imaging microscope. Color images were captured with a Photometric CoolSNAP™$_{HQ}$ CCD camera at 1392×1040 resolution. Low power images were generated with a 40X acroplan objective using the RS Image™ 1.9.2 software.

**1.4.2.1. NT immunoreactivity in sciatic nerve, grey matter of spinal cord, and DRG neurons:** NT immunoreactivities in the sciatic nerve, grey matter of spinal cord, and dorsal root ganglion neurons were assessed by immunofluorescent histochemistry. In brief, sections were deparaffinized in xylene, hydrated in decreasing concentrations of ethanol and washed in water. For immunofluorescent histochemistry, rabbit polyclonal anti-NT antibody was used in a working dilution 1:400. Secondary Alexa Fluor 488 goat anti-rabbit antibody was applied in a working dilution 1:200. Negative controls for non-specific staining were processed without primary antibody. Sections were mounted in Prolong Gold Antifade Reagent. The intensity of fluorescence was graded from 1 to 4 (1 — no staining; 2 — faint; 3 — moderate; 4 — intense), and the immunohistochemistry score was expressed as mean±SEM for each experimental group.

**1.4.2.2. Poly(ADP-ribose) immunoreactivity:** Poly(ADP-ribose) immunoreactivity was assessed as described (Garcia Soriano et al., 2001; Obrosova et al., 2004, 2005a) with minor modifications. In brief, sections were deparaffinized in xylene, hydrated in decreasing concentrations of ethanol and washed in water. Non-specific binding was blocked with the mouse IG blocking reagent supplied with the Vector M.O.M. Basic Immunodetection Kit. Then mouse monoclonal anti-poly(ADP-ribose) antibody was diluted 1:100 in 1% BSA in TBS, and applied overnight at 4 °C in the humidity chamber. Secondary Alexa Fluor 488 goat anti-mouse antibody was diluted 1:200 in TBS and applied for 2 h at room temperature. Sections were mounted in Prolong Gold Antifade Reagent. At least, ten fields of each section were examined to select one representative image. Representative images were microphotographed, and the number of poly(ADP-ribose)-positive nuclei calculated for each microphotograph.

**1.4.2.3. Intraepidermal nerve fiber density (INFD):** INFD was assessed as described (Malmberg et al., 2004) with minor modification. Three randomly chosen 5 μm sections from each mouse were deparaffinized in xylene, hydrated in decreasing concentrations of ethanol and washed in water. Non-specific binding was blocked by 10% goat serum containing 1% BSA in TBS (DAKO, Carpinteria, CA) for 2 h, and the Avidin/Biotin Blocking kit, according to the manufacturer's instructions. Then, rabbit polyclonal anti-protein gene product 9.5 (ubiquitin c-terminal hydrolase) antibody was applied in 1:2000 dilution. Secondary biotinylated goat anti-rabbit IgG (H + L) antibody was applied in 1:400 dilution, and the staining performed with the VECTASTAIN Elite ABC Kit (Standard*). For visualization of specific binding sites, the DAB Substrate Kit containing 3,3-diaminobenzidine was used.

Sections were counterstained with Gill's hematoxylin, dehydrated and mounted in Micromount mounting medium (Surgipath Medical Ind., Richmond, IL). Intraepidermal nerve fiber profiles were counted blindly by three independent investigators, under an Olympus BX-41 microscope, and the average values were used. Microphotographs of stained sections were taken on Axioscop 2 microscope (Zeiss) at 4× magnification, and the length of epidermis was assessed with the ImagePro 3.0 program (Media Cybernetics). An average of 2.8 ± 0.3 mm of the sample length was investigated to calculate a number of nerve fiber profiles per mm of epidermis.

### 1.5. Statistical analysis

The results are expressed as mean ± SEM. Data were subjected to equality of variance *F* test, and then to log transformation, if necessary, before one-way analysis of variance. Where overall significance ($p<0.05$) was attained, individual between-group comparisons were made using the Student–Newman–Keuls multiple range test. Significance was defined at $p<0.05$. When between-group variance differences could not be normalized by log transformation (datasets for body weights and plasma glucose), the data were analyzed by the nonparametric Kruskal–Wallis one-way analysis of variance, followed by the Bonferroni/Dunn test for multiple comparisons.

## 2. Results

Whereas initial body weights were similar in control and diabetic mice, final body weights were 14% lower in the diabetic group ($p<0.01$, Table 1). Initial (after STZ injection) blood glucose concentrations were 82% higher in diabetic mice compared with controls. Hyperglycemia progressed with the prolongation of diabetes, and the difference between final blood glucose concentrations in the two groups exceeded 4-fold. A peroxynitrite decomposition catalyst treatment did not affect weight gain or blood glucose concentrations in either control or diabetic mice.

The latency of hind paw withdrawal in response to radiant heat was increased by 103% in mice with 6-week duration of diabetes compared with the control group ($p<0.01$), indicative of clearly manifest thermal hypoalgesia (Fig. 1, A). This is in agreement with the results of tail-flick and hot plate tests which also revealed increased thermal response latencies in this diabetic group (Fig. 2, B and C). All three tests detected virtually identical responses to thermal noxious stimuli in untreated and a peroxynitrite decomposition catalyst-treated non-diabetic mice. FP15 therapy alleviated, but not completely prevented, diabetes-associated thermal hypoalgesia registered by paw withdrawal and tail-flick tests. In the hot plate test, thermal response latencies in peroxynitrite decomposition catalyst-treated diabetic mice and the control group did not differ significantly ($p=0.09$).

Diabetic mice with 6-week duration of STZ-diabetes also had mechanical hypoalgesia detected with the tail pressure Randall–Sellito test (Fig. 2, A). The tail pressure threshold was increased by 19% in diabetic mice compared with the control group. A peroxynitrite decomposition catalyst tended to reduce mechanical hypoalgesia in diabetic mice (to 113% of the control value, $p<0.05$ vs controls and $>0.05$ vs untreated diabetic group), without affecting the tail pressure threshold in control mice. Another sensory abnormality developing in diabetic mice was tactile allodynia. Tactile withdrawal threshold in response to light touch with flexible von Frey filaments was reduced by 69% in diabetic mice compared with controls ($p<0.01$). A peroxynitrite decomposition catalyst treatment tended to increase tactile withdrawal threshold in diabetic mice but the difference with the corresponding untreated group did not achieve statistical significance ($p<0.01$ vs controls and $p=0.17$ vs untreated diabetic group). The agent did not affect this variable in control mice.

INFD was reduced by 38% in diabetic mice compared with controls ($p<0.01$, Fig. 3). FP15 tended to increase INFD in diabetic mice, but the difference with the corresponding untreated group did not achieve statistical significance ($p<0.05$ vs controls and $p=0.054$ vs untreated diabetic group). A peroxynitrite decomposition catalyst treatment did not affect INFD in control mice.

NT immunofluorescence was increased by 87% in the sciatic nerve of diabetic mice compared with the control group (Fig. 4, A and B). A peroxynitrite decomposition catalyst treatment did not affect NT immunofluorescence in control mice, and essentially reduced ($p<0.05$ vs controls, and <0.01 vs untreated diabetic group) this variable in diabetic mice. The number of sciatic nerve poly(ADP-ribose)-positive nuclei was increased by 103% in diabetic mice compared with controls ($p<0.01$, Fig. 4, C and D). No significant difference in the numbers of sciatic nerve poly (ADP-ribose)-positive nuclei was found between FP15-treated diabetic mice and the control group. A peroxynitrite decomposition catalyst did not affect poly(ADP-ribose) immunofluorescence in control mice.

The similar patterns were observed in the grey matter of spinal cord (Fig. 5) and DRGs (Fig. 6). In the grey matter of spinal cord, NT immunofluorescence and the number of poly(ADP-ribose)-positive nuclei were increased by 203% and 157%, respectively, in diabetic mice compared with the control group ($p<0.01$ for both comparisons). FP15 treatment did not affect NT and poly (ADP-ribose) immunofluorescence in the grey matter of spinal cord in control mice. The agent completely normalized NT immunofluorescence and essentially reduced, but completely not normalized, the number of poly(ADP-ribose)-positive nuclei in diabetic mice.

NT immunofluorescence in DRG neurons was increased by 60% in diabetic mice compared with the control group ($p<0.01$, Fig. 6, A and B). The total number of DRG poly(ADP-ribose)-positive nuclei was 22% higher in diabetic than in control mice ($p<0.05$), with poly(ADP-ribose) immunofluorescence localized primarily in satellite cells (Fig. 6, C and D). The percentage of DRG neurons with weak and moderate poly(ADP-ribose) immunofluorescence was lower in diabetic mice compared with the control group; the reverse was observed for DRG neurons with intense poly(ADP-ribose) immunofluorescence (Fig. 6, E and F). The peroxynitrite decomposition catalyst treatment did not affect neuronal NT immunofluorescence and the total number of DRG poly(ADP-ribose)-positive nuclei in control mice, but significantly reduced these two variables in diabetic mice ($p<0.05$ for both comparisons). The percentage of DRG neurons with intense poly(ADP-ribose) immunofluorescence was reduced and of those with weak and moderate immunofluorescence increased in FP15-treated diabetic mice compared with the corresponding untreated group. The peroxynitrite decomposition catalyst did not affect the percent distribution of DRG neurons with weak, moderate and intense poly(ADP-ribose) immunofluorescence in control mice.

## 3. Discussion

Sensory neuropathy seriously affects the quality of life of a significant number of patients with diabetes mellitus. To date, the pathogenetic mechanisms of this complication have not been properly elucidated. Studies of behavioral responses to external stimuli in diabetic rats and mice provided somewhat contradictory information regarding manifestations of abnormal sensation and pain in animal models of diabetes and identified a number of biochemical mechanisms underlying diabetic sensory neuropathy (Calcutt, 2002, 2004).

The paw withdrawal and tail-flick tests detecting the time to movement of a hindpaw or tail from a noxious heat source (Calcutt, 2002, 2004) revealed hyperalgesia in STZ-diabetic and Zucker diabetic fatty rats with short-term diabetes (Calcutt et al., 2004; Cameron et al., 2001a,b; Cotter et al., 2002; Ilnytska et al., 2006; Stevens et al., 2007), and hypoalgesia in

STZ-diabetic and Zucker diabetic fatty rats with longer durations of diabetes (Calcutt et al., 2004; Obrosova et al., in press), as well as STZ-diabetic (Obrosova et al., 2005b), NOD (Obrosova et al., 2005b), and leptin-deficient *ob/ob* mice (Drel et al., 2006a). Note that thermal hyperalgesia is sometimes observed in human subjects in the initial phase of diabetes mellitus (Dyck et al., 2000), whereas advanced clinical PDN is characterized by increased thermal perception thresholds (hypoalgesia) that progress to sensory loss, occurring in conjunction with degeneration of all types of peripheral nerve fibers (Calcutt, 2002, 2004). Thus, identification of the mechanisms underlying both thermal hyper- and hypoalgesia is clinically relevant. Numerous pharmacological studies in animal models have been performed to sort out the involvement of the key hyperglycemia-induced biochemical mechanisms in diabetes-associated changes in thermal nociception. Aldose reductase inhibitors (ARIs, Calcutt et al., 2004), antioxidants *i.e.*, taurine (Li et al., 2005b), α-lipoic acid (Cameron et al., 2001a), the hydroxyl radical scavenger dimethylthiourea (Cameron et al., 2001b), as well as the protein kinase C inhibitor LY333531 (Cotter et al., 2002), the PARP inhibitor 1,5-isoqunolinediol (Ilnytska et al., 2006) and PARP inhibitor-containing combination therapies (Li et al., 2005a), have been found to prevent or correct thermal hyperalgesia in STZ-diabetic rats. Taurine prevented thermal hyperalgesia in ZDF rats (Li et al., 2006). Insulin therapy resulting in achievement of protracted normoglycemia (Calcutt, 2002, 2004), ARIs (Calcutt et al., 2004), Schwann cell-derived ciliary neurotrophic factor (CNTF) (Calcutt et al., 2004), the neurotrophic peptide deriving from prosaposin, TX14(A), (Calcutt et al., 2000), and a sonic hedgehog–IgG fusion protein (Calcutt et al., 2003), as well as PARP inhibitors (Obrosova et al., 2007a) prevented or alleviated thermal hypoalgesia in STZ-diabetic rats with longer duration of diabetes. Thus, pharmacological studies in diabetic animal models revealed importance of hyperglycemia, increased aldose reductase and protein kinase C activities, impaired neurotrophic support, as well as oxidative stress and PARP activation, in thermal hyper- and hypoalgesia associated with PDN. Taking into consideration, that hyperglycemia as well as AR and PARP activation lead to enhanced nitrotyrosine formation in tissue sites for diabetic complications (Cheung et al., 2005; Drel et al., 2006b; El-Remessy et al., 2003; Ho et al., 2006; Obrosova et al., 2005c) including PNS (Ho et al., 2006; Obrosova et al., 2005a,c; Szabo et al., 2006), these findings are quite consistent with the present study implicating nitrosative stress in thermal hypoalgesia in STZ-diabetic mice. Note, that oxidative stress leads to peroxynitrite formation both directly (reaction between superoxide and nitric oxide) and indirectly, *via* downregulation of superoxide dismutase and resultant impairment of superoxide anion radical neutralization (Stevens et al., 2000). Neurotrophic factor deficit is also known to promote increased superoxide generation in PNS (Li et al., 1998).

Another phenomenon, mechanical hyperalgesia, detected by reduced paw withdrawal thresholds during paw stimulation with rigid von Frey filaments or Randall–Sellito test, has been found clearly manifest in STZ-diabetic and ZDF rats (Cameron et al., 2001a,b; Cotter et al., 2002; Ilnytska et al., 2006; Li et al., 2006), and reversed or alleviated by antioxidants including α-lipoic acid (Cameron et al., 2001a), dimethylthiourea (Cameron et al., 2001b), taurine (Li et al., 2005b) as well as PARP inhibitors (Ilnytska et al., 2006). Of interest, STZ-diabetic mice develop mechanical hypo-, rather than hyperalgesia, *i.e.* the condition consistent with sensory loss in human subjects with advanced PDN. The findings of the present study suggest that RNS contribute to the development of diabetes-associated mechanical hypoalgesia. This effect could at least partially be due to resultant PARP activation as STZ-diabetic PARP-deficient mice did not develop mechanical hypoalgesia that was clearly manifest in diabetic wild-type mice (Obrosova et al., 2007a).

Painful diabetic neuropathy in human subjects is sometimes complicated by tactile allodynia, a condition where light touch is perceived as painful (Calcutt, 2002, 2004). Clearly manifest tactile allodynia is observed in STZ-diabetic rats (Calcutt et al., 2004; Ilnytska et al., 2006) and mice (the present study). The mechanisms of this phenomenon are not well understood.

Tactile allodynia in diabetic rats has been prevented or reversed by protracted insulin therapy (Calcutt, 2002, 2004), the inhibitor of catechol-*O*-methyltransferase and antioxidant nitecapone (Pertovaara et al., 2001), and the PARP inhibitor 1,5-isoquinolinediol (Ilnytska et al., 2006). A peroxynitrite decomposition catalyst treatment tended to increase tactile response thresholds in STZ-diabetic and *ob/ob* mice (the present study, and Vareniuk et al., 2007), and did increase tactile response thresholds in STZ-diabetic rats (Obrosova et al., unpublished). However, tactile response thresholds in peroxynitrite decomposition catalyst-treated STZ-diabetic rats (Obrosova et al., unpublished) and STZ-diabetic and *ob/ob* mice (Vareniuk et al., 2007) remained 1.5–2.5-fold lower than in the corresponding non-diabetic controls which suggests that the contribution of RNS diabetes-associated tactile allodynia is fairly minor.

Theoretically, nitrosative stress can contribute to diabetic sensory neuropathy *via* several mechanisms and, in particular, impairment in neurotrophic support and PARP activation (Obrosova et al., 2005b; Pacher et al., 2005; Szabo et al., 2002a). As indicated above, neurotrophic factors as well as PARP inhibitors prevented thermal hypoalgesia in STZ-diabetic rats (Calcutt et al., 2000, 2004; Obrosova et al., 2007a). PARP inhibition counteracted thermal hypoalgesia, mechanical hyperalgesia, and tactile allodynia in rats with 12-week duration of STZ-diabetes (Obrosova et al., 2007a). Furthermore, these disorders did not develop in STZ-diabetic PARP-deficient mice being clearly manifest in diabetic PARP+/+ mice (Obrosova et al., 2006).

Recent development of techniques for assessment small-caliber nerve fiber degeneration *i.e.*, corneal confocal microscopy, an *in vivo* imaging technique for quantitative assessment of degeneration and regeneration of corneal nerve fibers (Malik et al., 2003), and skin biopsy with quantitation of epidermal nerve fibers (Pittenger et al., 2004; Sumner et al., 2003), stimulated studies of this phenomenon in animal models (Christianson et al., 2003; Drel et al., 2006a; Toth et al., 2006) and human subjects with PDN (Pittenger et al., 2004; Sumner et al., 2003). Note, that physiological correlates of intraepidermal nerve fiber loss in animal models of diabetes remain to be established as several studies (Christianson et al., 2003; Vareniuk et al., 2007) suggest that neither thermal or mechanical hypoalgesia nor their amelioration by a pharmacological treatment necessarily parallel small sensory nerve fiber degeneration or regeneration. In the present study, the mice with 3-week duration of STZ-diabetes had thermal and mechanical hypoalgesia, but no intraepidermal nerve fiber loss. The mice with 6-week duration of STZ-diabetes displayed ~38% epidermal nerve fiber loss, which showed a trend towards alleviation with FP15 treatment but the difference with the untreated groups did not achieve statistical significance ($p$ =0.054). Note, that a significant ($p$<0.05) increase in intra-epidermal nerve fiber density was achieved in STZ-diabetic mice treated with 5 mg $kg^{-1}$ $day^{-1}$ and 10 mg $kg^{-1}$ $day^{-1}$ of another peroxynitrite decomposition catalyst, Fe(III) tetramesitylporphyrin octasulfonate (Pavlov et al., 2007). Furthermore, whereas PARP+/+ mice with 10-week duration of STZ-diabetes displayed ~53% intraepidermal nerve fiber loss, diabetic PARP−/− preserved completely normal intraepidermal nerve fiber density (Obrosova et al., 2007a). The latter supports the important role of nitrosative stress in small sensory nerve fiber degeneration associated with PDN, because peroxynitrite provides a major contribution to PARP activation in tissues-sites for diabetic complications including PNS (Obrosova et al., 2005b; Pacher et al., 2005; Szabo et al., 2002a). In the present study, PARP activation in peripheral nerve, spinal cord and DRG neurons and satellite cells was markedly reduced in FP15-treated diabetic mice compared with the corresponding untreated group.

In conclusion, nitrosative stress plays an important role in sensory neuropathy in streptozotocin-diabetic mice. The results provide the rationale for development of peroxynitrite decomposition catalysts for prevention and treatment of sensory disorders in human subjects with diabetes mellitus.

**Acknowledgements**

This study was supported by the American Diabetes Association Research Grant 7-05-RA-102, the Juvenile Diabetes Research Foundation International Grant 1-2005-223, the National Institutes of Health Grant DK 071566-01 (all to I.G.O.), and the Intramural Research Program of the National Institutes of Health/National Institute of Alcohol Abuse and Alcoholism (to P.P.). Metalloporphyrin synthesis was supported by the National Institutes of Health Grant GM 36298 and the New Jersey Commission on Science and Technology (both to JTG). The authors thank Nazar Mashtalir and Jeho Shin for expert technical assistance.

## References

Calcutt NA. Potential mechanisms of neuropathic pain in diabetes. Int Rev Neurobiol 2002;50:205–228. [PubMed: 12198811]

Calcutt NA. Modeling diabetic sensory neuropathy in rats. Methods Mol Med 2004;99:55–65. [PubMed: 15131329]

Calcutt NA, Freshwater JD, O'Brien JS. Protection of sensory function and antihyperalgesic properties of a prosaposin-derived peptide in diabetic rats. Anesthesiology 2000;93:1271–1278. [PubMed: 11046216]

Calcutt NA, Allendoerfer KL, Mizisin AP, Middlemas A, Freshwater JD, Burgers M, Ranciato R, Delcroix JD, Taylor FR, Shapiro R, Strauch K, Dudek H, Engber TM, Galdes A, Rubin LL, Tomlinson DR. Therapeutic efficacy of sonic hedgehog protein in experimental diabetic neuropathy. J Clin Invest 2003;111:507–514. [PubMed: 12588889]

Calcutt NA, Freshwater JD, Mizisin AP. Prevention of sensory disorders in diabetic Sprague–Dawley rats by aldose reductase inhibition or treatment with ciliary neurotrophic factor. Diabetologia 2004;47:718–724. [PubMed: 15298349]

Cameron NE, Jack AM, Cotter MA. Effect of alpha-lipoic acid on vascular responses and nociception in diabetic rats. Free Radic Biol Med 2001a;31:125–135. [PubMed: 11425498]

Cameron NE, Tuck Z, McCabe L, Cotter MA. Effect of the hydroxyl radical scavenger, dimethylthiourea, on peripheral nerve tissue perfusion, conduction velocity and nociception in experimental diabetes. Diabetologia 2001b;44:1161–1169. [PubMed: 11596672]

Cheng C, Zochodne DW. Sensory neurons with activated caspase-3 survive long-term experimental diabetes. Diabetes 2003;52:2363–2371. [PubMed: 12941777]

Cheung AK, Fung MK, Lo AC, Lam TT, So KF, Chung SS, Chung SK. Aldose reductase deficiency prevents diabetes-induced blood-retinal barrier breakdown, apoptosis, and glial reactivation in the retina of db/db mice. Diabetes 2005;54:3119–3125. [PubMed: 16249434]

Christianson JA, Riekhof JT, Wright DE. Restorative effects of neurotrophin treatment on diabetes-induced cutaneous axon loss in mice. Exp Neurol 2003;179:188–199. [PubMed: 12618126]

Coppey LJ, Gellett JS, Davidson EP, Dunlap JA, Lund DD, Yorek MA. Effect of antioxidant treatment of streptozotocin-induced diabetic rats on endoneurial blood flow, motor nerve conduction velocity, and vascular reactivity of epineurial arterioles of the sciatic nerve. Diabetes 2001;50:1927–1937. [PubMed: 11473057]

Cotter MA, Jack AM, Cameron NE. Effects of the protein kinase C beta inhibitor LY333531 on neural and vascular function in rats with streptozotocin-induced diabetes. Clin Sci (Lond) 2002;103:311–321. [PubMed: 12193157]

Drel VR, Mashtalir N, Ilnytska O, Shin J, Li F, Lyzogubov VV, Obrosova IG. The leptin-deficient (*ob/ob*) mouse: a new animal model of peripheral neuropathy of type 2 diabetes and obesity. Diabetes 2006a;55:3335–3343. [PubMed: 17130477]

Drel VR, Pacher P, Stevens MJ, Obrosova IG. Aldose reductase inhibition counteracts nitrosative stress and poly(ADP-ribose) polymerase activation in diabetic rat kidney and high-glucose-exposed human mesangial cells. Free Radic Biol Med 2006b;40:1454–1465. [PubMed: 16631535]

Dyck PJ, Dyck PJ, Larson TS, O'Brien PC, Velosa JA. Patterns of quantitative sensation testing of hypoesthesia and hyperalgesia are predictive of diabetic polyneuropathy: a study of three cohorts. Nerve growth factor study group. Diabetes Care 2000;23:510–517. [PubMed: 10857944]

El-Remessy AB, Abou-Mohamed G, Caldwell RW, Caldwell RB. High glucose-induced tyrosine nitration in endothelial cells: role of eNOS uncoupling and aldose reductase activation. Invest Ophthalmol Vis Sci 2003;44:3135–3143. [PubMed: 12824263]

Frustaci A, Kajstura J, Chimenti C, Jakoniuk I, Leri A, Maseri A, Nadal-Ginard B, Anversa P. Myocardial cell death in human diabetes. Circ Res 2000;87:1123–1132. [PubMed: 11110769]

Garcia Soriano F, Virag L, Jagtap P, Szabo E, Mabley JG, Liaudet L, Marton A, Hoyt DG, Murthy KG, Salzman AL, Southan GJ, Szabo C. Diabetic endothelial dysfunction: the role of poly(ADP-ribose) polymerase activation. Nat Med 2001;7:108–113. [PubMed: 11135624]

Ho EC, Lam KS, Chen YS, Yip JC, Arvindakshan M, Yamagishi S, Yagihashi S, Oates PJ, Ellery CA, Chung SS, Chung SK. Aldose reductase-deficient mice are protected from delayed motor nerve conduction velocity, increased c-Jun NH2-terminal kinase activation, depletion of reduced glutathione, increased superoxide accumulation, and DNA damage. Diabetes 2006;55:1946–1953. [PubMed: 16804062]

Hoeldtke, RD. Nitrosative stress in early Type 1 diabetes, Streeten Memorial Lecture. In: David, HP., editor. Clin Auton Res. 13. 2003. p. 406-421.

Ilnytska O, Lyzogubov VV, Stevens MJ, Drel VR, Mashtalir N, Pacher P, Yorek MA, Obrosova IG. Poly (ADP-ribose) polymerase inhibition alleviates experimental diabetic sensory neuropathy. Diabetes 2006;55:1686–1694. [PubMed: 16731831]

Li XM, Juorio AV, Qi J, Boulton AA. L-deprenyl potentiates NGF-induced changes in superoxide dismutase mRNA in PC12 cells. J Neurosci Res 1998;53:235–238. [PubMed: 9671980]

Li F, Drel VR, Szabo C, Stevens MJ, Obrosova IG. Low-dose poly(ADP-ribose) polymerase inhibitor-containing combination therapies reverse early peripheral diabetic neuropathy. Diabetes 2005a; 54:1514–1522. [PubMed: 15855340]

Li F, Obrosova IG, Abatan O, Tian D, Larkin D, Stuenkel EL, Stevens MJ. Taurine replacement attenuates hyperalgesia and abnormal calcium signaling in sensory neurons of STZ-D rats. Am J Physiol, Endocrinol Metabol Gastrointest Physiol 2005b;288:E29–E36.

Li F, Abatan OI, Kim H, Burnett D, Larkin D, Obrosova IG, Stevens MJ. Taurine reverses neurological and neurovascular deficits in Zucker diabetic fatty rats. Neurobiol Dis 2006;22:669–676. [PubMed: 16624563]

Mabley JG, Liaudet L, Pacher P, Southan GJ, Groves JT, Salzman AL, Szabo C. Part II: beneficial effects of the peroxynitrite decomposition catalyst FP15 in murine models of arthritis and colitis. Mol Med 2002;8:581–590. [PubMed: 12477968]

Malik RA, Kallinikos P, Abbott CA, van Schie CH, Morgan P, Efron N, Boulton AJ. Corneal confocal microscopy: a non-invasive surrogate of nerve fibre damage and repair in diabetic patients. Diabetologia 2003;46:683–688. [PubMed: 12739016]

Malmberg AB, Mizisin AP, Calcutt NA, von Stein T, Robbins WR, Bley KR. Reduced heat sensitivity and epidermal nerve fiber immunostaining following single applications of a high-concentration capsaicin patch. Pain 2004;111:360–367. [PubMed: 15363880]

Nangle MR, Cotter MA, Cameron NE. Effects of the peroxynitrite decomposition catalyst, FeTMPyP, on function of corpus cavernosum from diabetic mice. Eur J Pharmacol 2004;502:143–148. [PubMed: 15464100]

Obrosova IG, Li F, Abatan OI, Forsell MA, Komjati K, Pacher P, Szabo C, Stevens MJ. Role of poly (ADP-ribose) polymerase activation in diabetic neuropathy. Diabetes 2004;53:711–720. [PubMed: 14988256]

Obrosova IG, Drel VR, Pacher P, Ilnytska O, Wang ZQ, Stevens MJ, Yorek MA. Oxidative-nitrosative stress and poly(ADP-ribose) polymerase (PARP) activation in experimental diabetic neuropathy: the relation is revisited. Diabetes 2005a;54:3435–3441. [PubMed: 16306359]

Obrosova IG, Mabley JG, Zsengeller Z, Charniauskaya T, Abatan OI, Groves JT, Szabo C. Role for nitrosative stress in diabetic neuropathy: evidence from studies with a peroxynitrite decomposition catalyst. FASEB J 2005b;19:401–403. [PubMed: 15611153]

Obrosova IG, Pacher P, Szabo C, Zsengeller Z, Hirooka H, Stevens MJ, Yorek MA. Aldose reductase inhibition counteracts oxidative-nitrosative stress and poly(ADP-ribose) polymerase activation in tissue sites for diabetes complications. Diabetes 2005c;54:234–242. [PubMed: 15616034]

Obrosova IG, Ilnytska O, Lyzogubov V, Drel VR, Mashtalir N, Pacher P, Stevens MJ, Yorek MA. Poly (ADP-ribose) polymerase-1 (PARP) activation and diabetic sensory neuropathy. Diabetes 2006;55 (Suppl 1):A38.Abstract

Obrosova IG, Lyzogubov VV, Ilnytska O, Mashtalir N, Vareniuk I, Pavlov I, Xu W, Zhang J, Drel VR. PARP inhibition or gene deficiency counteract intraepidermal nerve fiber loss and neuropathic pain associated with Type 1 diabetes. Diabetes 2007a;56(Suppl 1):A1.Abstract

Obrosova IG, Ilnytska O, Lyzogubov V, Mashtalir M, Nadler JL, Drel CR. High fat diet-induced neuropathy of prediabetes and obesity: effects of “healthy” diet and aldose reductase inhibition. Diabetes 2007b;56(Suppl 1):A207.

Olcott AP, Tocco G, Tian J, Zekzer D, Fukuto J, Ignarro L, Kaufman DL. A salen-manganese catalytic free radical scavenger inhibits type 1 diabetes and islet allograft rejection. Diabetes 2004;53:2574–2580. [PubMed: 15448086]

Oltman CL, Coppey LJ, Gellett JS, Davidson EP, Lund DD, Yorek MA. Progression of vascular and neural dysfunction in sciatic nerves of Zucker diabetic fatty and Zucker rats. Am J Physiol, Endocrinol Metabol Gastrointest Physiol 2005;289:E113–E122.

Pacher P, Liaudet L, Bai P, Mabley JG, Kaminski PM, Virag L, Deb A, Szabo E, Ungvari Z, Wolin MS, Groves JT, Szabo C. Potent metalloporphyrin peroxynitrite decomposition catalyst protects against the development of doxorubicin-induced cardiac dysfunction. Circulation 2003;107:896–904. [PubMed: 12591762]

Pacher P, Obrosova IG, Mabley JG, Szabo C. Role of nitrosative stress and peroxynitrite in the pathogenesis of diabetic complications. Emerging new therapeutical strategies. Curr Med Chem 2005;12:267–275. [PubMed: 15723618]

Pacher P, Beckman JS, Liaudet L. Nitric oxide and peroxynitrite in health and disease. Physiol Rev 2007;87:315–424. [PubMed: 17237348]

Pavlov I, Vareniuk I, Drel VR, Lyzogubov VV, Ilnytska O, Mashtalir N, Tibrewala J, Groves JT, Obrosova IG. Nitrosative stress and neuropathy in mouse models of Type 1 and Type 2 diabetes. Diabetes 2007;56(Suppl 1):A207.

Pertovaara A, Wei H, Kalmari J, Ruotsalainen M. Pain behavior and response properties of spinal dorsal horn neurons following experimental diabetic neuropathy in the rat: modulation by nitecapone, a COMT inhibitor with antioxidant properties. Exp Neurol 2001;167:425–434. [PubMed: 11161631]

Pittenger G, Burkus N, McNulty P, Basta B, Vinik A. Intraepidermal nerve fibers are indicators of small fiber neuropathy in both diabetic and non-diabetic patients. Diabetes Care 2004;27:1974–1979. [PubMed: 15277426]

Sumner CJ, Sheth S, Griffin JW, Cornblath DR, Polydefkis M. The spectrum of neuropathy in diabetes and impaired glucose tolerance. Neurology 2003;60:108–111. [PubMed: 12525727]

Stevens MJ, Obrosova I, Cao X, Van Huysen C, Greene DA. Effects of DL-alpha-lipoic acid on peripheral nerve conduction, blood flow, energy metabolism, and oxidative stress in experimental diabetic neuropathy. Diabetes 2000;49:1006–1015. [PubMed: 10866054]

Stevens MJ, Li F, Drel VR, Abatan OI, Kim H, Burnett D, Larkin D, Obrosova IG. Nicotinamide reverses neurological and neurovascular deficits in streptozotocin diabetic rats. J Pharmacol Exp Ther 2007;320:458–464. [PubMed: 17021258]

Szabo C, Mabley JG, Moeller SM, Shimanovich R, Pacher P, Virag L, Soriano FG, Van Duzer JH, Williams W, Salzman AL, Groves JT. Part I: pathogenetic role of peroxynitrite in the development of diabetes and diabetic vascular complications: studies with FP15, a novel potent peroxynitrite decomposition catalyst. Mol Med 2002a;8:571–580. [PubMed: 12477967]

Szabo C, Zanchi A, Komjati K, Pacher P, Krolewski AS, Quist WC, LoGerfo FW, Horton ES, Veves A. Poly(ADP-ribose) polymerase is activated in subjects at risk of developing type 2 diabetes and is associated with impaired vascular reactivity. Circulation 2002b;106:2680–2686. [PubMed: 12438293]

Szabo C, Biser A, Benko R, Bottinger E, Susztak K. Poly(ADP-ribose) polymerase inhibitors ameliorate nephropathy of type 2 diabetic Leprdb/db mice. Diabetes 2006;55:3004–3012. [PubMed: 17065336]

Thuraisingham RC, Nott CA, Dodd SM, Yaqoob MM. Increased nitrotyrosine staining in kidneys from patients with diabetic nephropathy. Kidney Int 2000;57:1968–1972. [PubMed: 10792615]

Toth C, Brussee V, Zochodne DW. Remote neurotrophic support of epidermal nerve fibres in experimental diabetes. Diabetologia 2006;49:1081–1088. [PubMed: 16528572]

Vareniuk I, Pavlov IA, Drel VR, Lyzogubov VV, Ilnytska O, Bell SR, Tibrewala J, Groves JT, Obrosova IG. Nitrosative stress and peripheral diabetic neuropathy in leptin-deficient (*ob/ob*) mice. Exp Neurol 2007;205:425–436. [PubMed: 17475250]

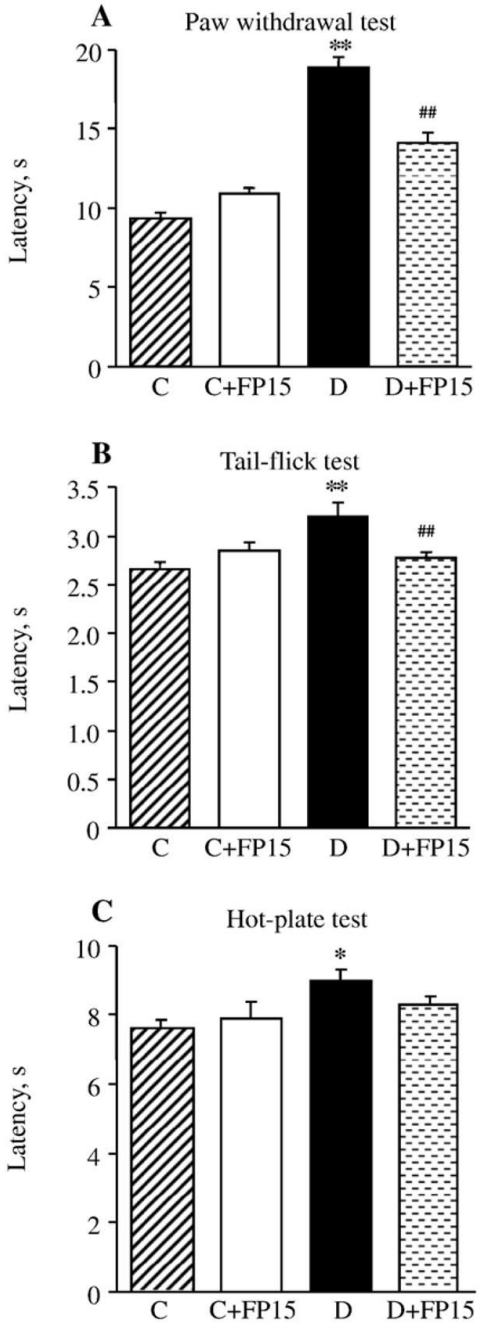


**Fig. 1.**

Paw withdrawal latencies in response to radiant heat (A), tail-flick test response latencies (B), and hot plate test response latencies (C) in control and diabetic mice with or without a peroxynitrite decomposition catalyst treatment. Mean ±SEM, $n$ =8–10 per group. C — control mice. D — diabetic mice. $^{a,b}p < 0.05$ and $< 0.01$ vs control mice; $^{d}p < 0.01$ vs untreated diabetic mice.

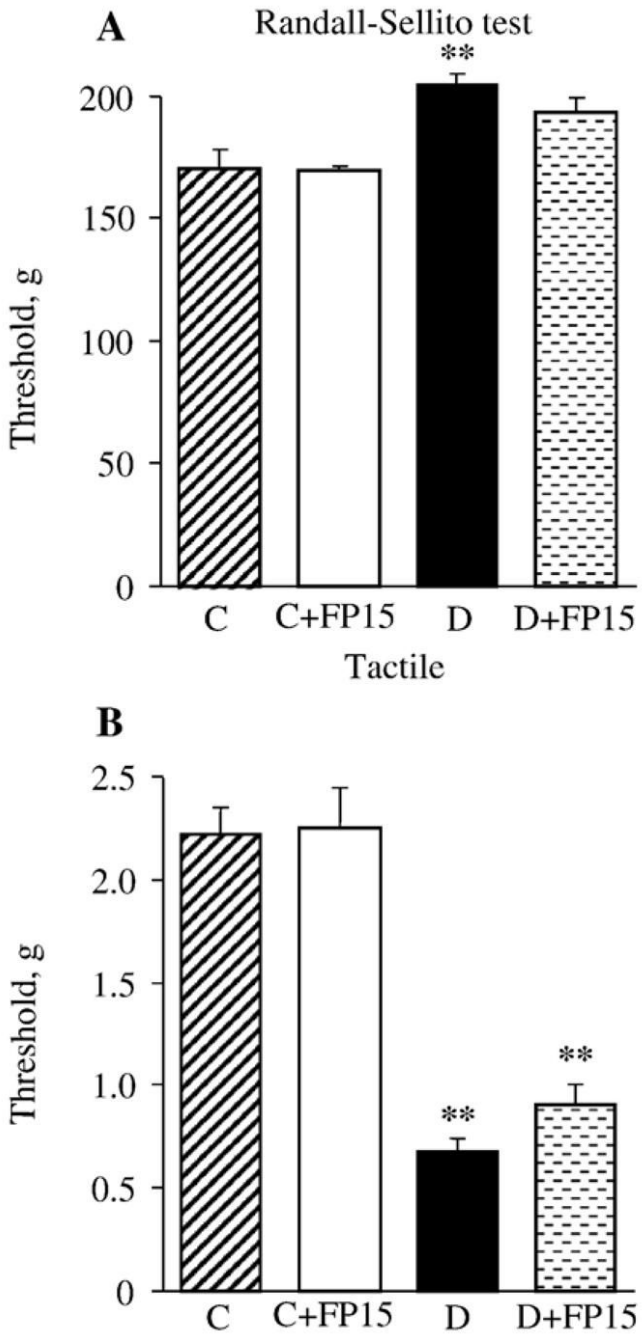


**Fig. 2.**

Mechanical withdrawal thresholds in tail pressure Randall–Sellito test (A) and tactile response thresholds in response to stimulation with flexible von Frey filaments (B) in control and diabetic mice with or without a peroxynitrite decomposition catalyst treatment. Mean±SEM, $n$=8–10 per group. C — control mice. D — diabetic mice. [b]$p< 0.05$ vs control mice.

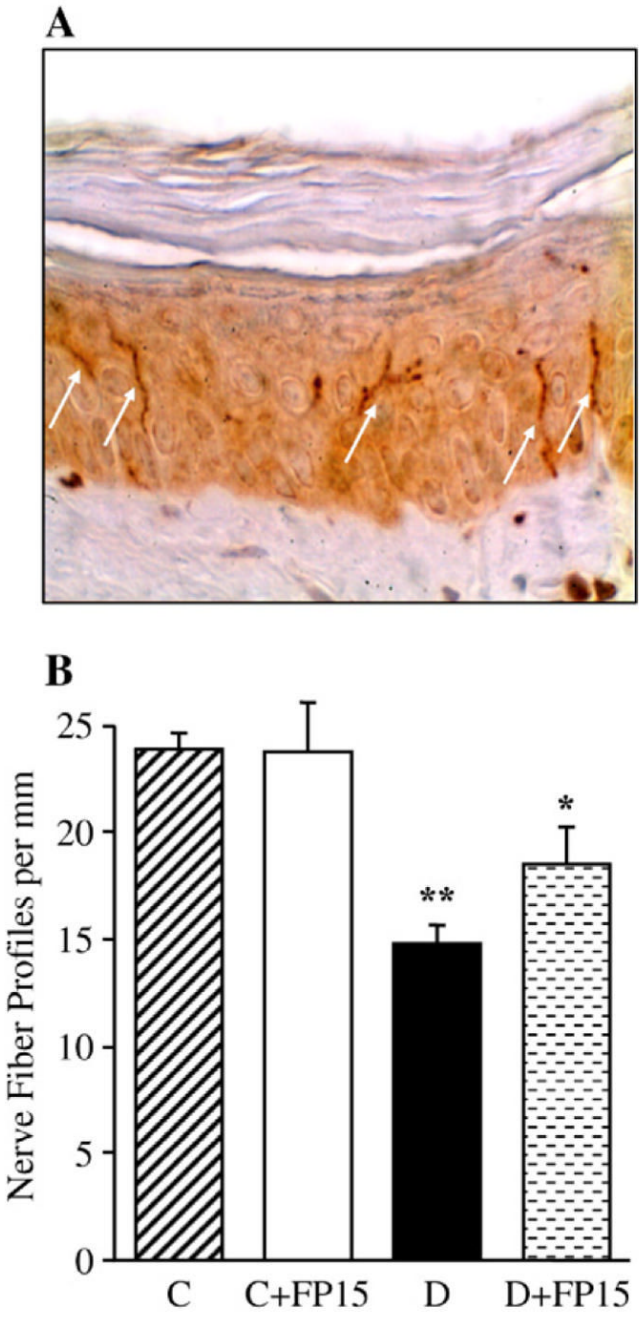


**Fig. 3.**

Intraepidermal nerve fiber profiles in control and diabetic mice with and without a peroxynitrite decomposition catalyst treatment. A — Representative image of intraepidermal nerve fiber profiles, magnification ×200; B — Skin fiber density. Mean±SEM, *n*=9–11 per group. C — control mice. D — diabetic mice. [a,b]*p*<0.05 and <0.01 vs control mice.

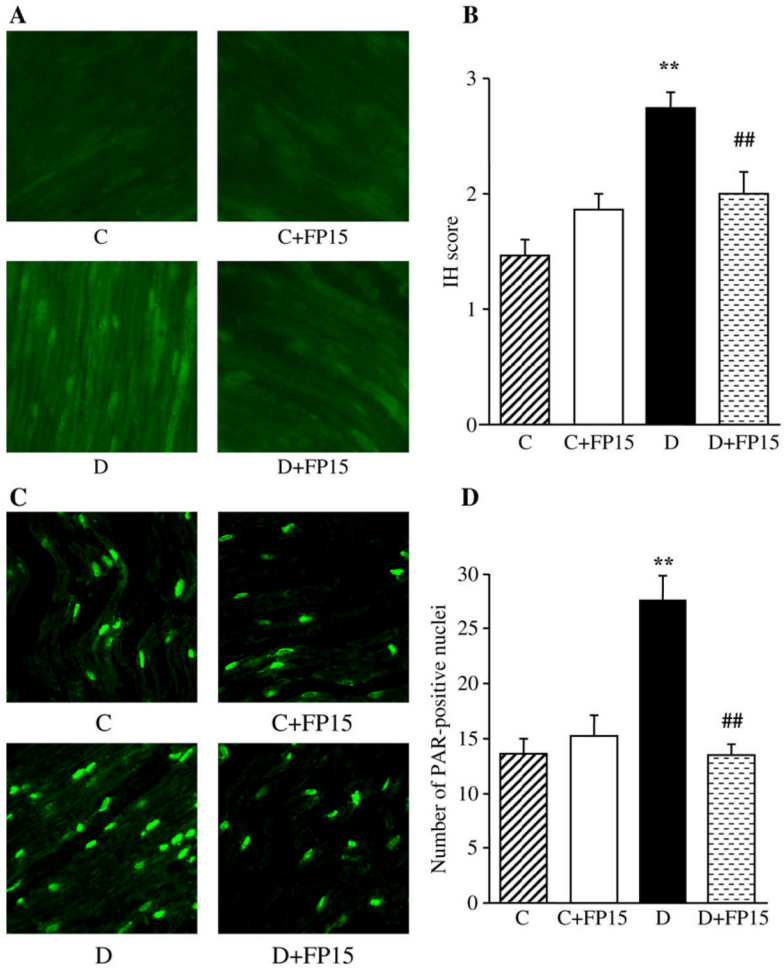


**Fig. 4.**

Representative microphotographs of immunofluorescent staining of nitrotyrosine (A) and poly (ADP-ribose) (C) in sciatic nerves of control and diabetic mice with and without a peroxynitrite decomposition catalyst treatment. Magnification ×40. Scores of nitrotyrosine immunofluorescence (B) and the numbers of poly(ADP-ribose)-positive nuclei (D) in sciatic nerves of control mice and diabetic mice with and without a peroxynitrite decomposition catalyst treatment. Mean±SEM, $n$=9–11 per group. C — control mice. D — diabetic mice. $^{b}p<0.01$ vs control mice; $^{d}p<0.01$ vs untreated diabetic mice.

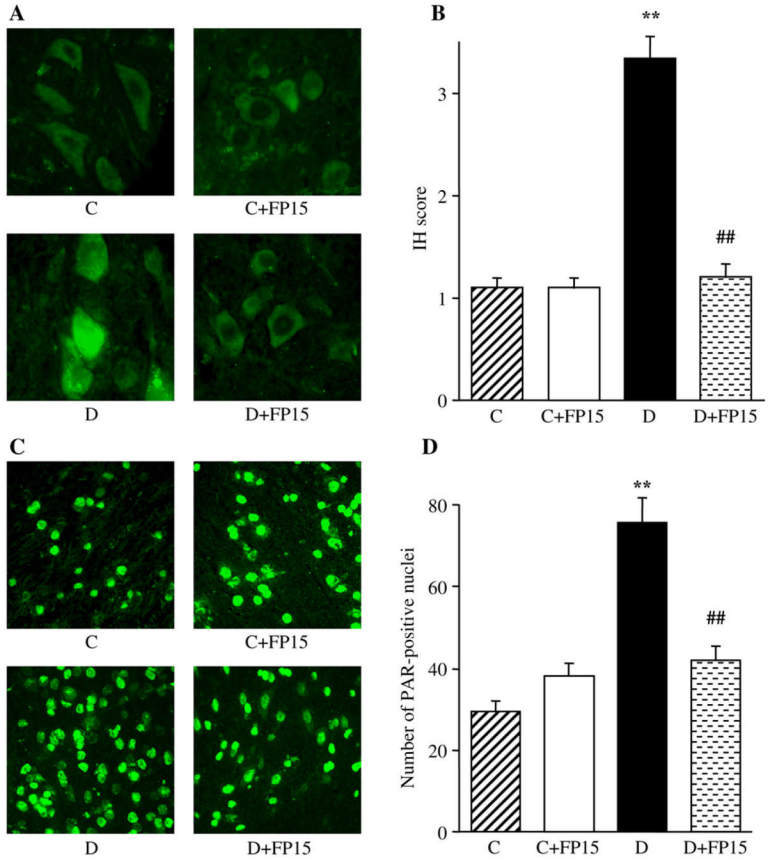


**Fig. 5.**

Representative microphotographs of immunofluorescent staining of nitrotyrosine (A) and poly (ADP-ribose) (C) in the grey matter of spinal cord of control mice and diabetic mice with and without a peroxynitrite decomposition catalyst treatment. Magnification ×40. Scores of nitrotyrosine immunofluorescence (B) and the numbers of poly(ADP-ribose)-positive nuclei (D) in the grey matter of spinal cord of control and diabetic mice with and without a peroxynitrite decomposition catalyst treatment. Mean±SEM, $n$=9–11 per group. C — control mice; D — diabetic mice. $^{b}p<0.01$ vs control mice; $^{d}p<0.01$ vs untreated diabetic mice.

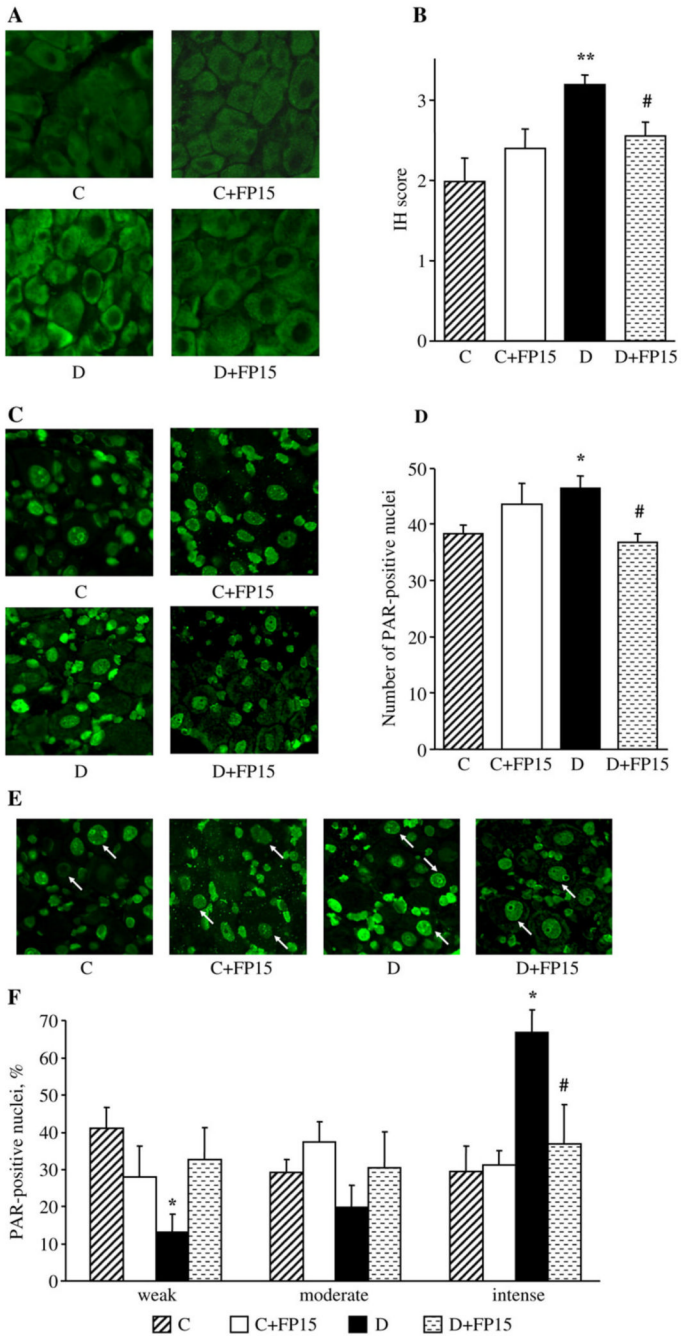


**Fig. 6.**

Representative microphotographs of immunofluorescent staining of nitrotyrosine (A) and poly (ADP-ribose) (C) in the dorsal root ganglia, and poly(ADP-ribose) in dorsal root ganglion neurons (E) of control and diabetic mice with and without a peroxynitrite decomposition catalyst treatment. Arrows on Fig. 6, E indicate neurons with identifiable poly(ADP-ribose) fluorescence. Magnification ×40. Scores of nitrotyrosine immunofluorescence in dorsal root ganglion neurons (B), counts of dorsal root ganglion poly(ADP-ribose)-positive nuclei (D), and percentage of dorsal root ganglion neurons with weak, moderate, and intense poly(ADP-ribose) immunofluorescence (F), in experimental groups. The number of dorsal root ganglion neurons with weak, moderate and intense poly(ADP-ribose) immunofluorescence was

expressed as a percentage of neurons with identifiable poly(ADP-ribose) immunofluorescence in the dorsal root ganglia of control and diabetic mice with and without a peroxynitrite decomposition catalyst treatment. Mean±SEM, $n$=9–11 per group. C — control mice; D — diabetic mice; [a,b]$p$<0.05 and <0.01 vs control mice; [c]$p$<0.05 vs untreated diabetic mice.

## Table 1

Initial and final body weights and blood glucose concentrations in control mice and diabetic mice with and without the peroxynitrite decomposition catalyst FP15 treatment

| | Body weight (g) | | Blood glucose (mmol/l) | |
|---|---|---|---|---|
| | **Initial** | **Final** | **Initial** | **Final** |
| Control | 20.6±0.40 | 29±0.95 | 7.9±0.17 | 8.0±0.2 |
| Control+FP15 | 19.8±0.33 | 27±0.81 | 8±0.2 | 7.9±0.12 |
| Diabetic | 20±0.3 | 25±0.5[a] | 14.4±0.7[a] | 33±0.2[a] |
| Diabetic+FP15 | 20.8±0.35 | 24.4±0.4[a] | 14.7±1.0[a] | 32.4±0.5[a] |

Data are means±SEM, $n$=9–11 per group.

[a] Significantly different from controls ($p$<0.01).